Calculating Radiation from Arbitrarily Shaped Aperture Antennas Using the Free Space Radiation Integrals

Adriaan J. Booysen

Antenna Systems Group
Saab Grintek Defence (Pty) Ltd.
Pretoria, South Africa
riaan.booysen@za.saabgroup.com

Abstract — A technique is derived by means of which the calculation of radiation from arbitrarily shaped aperture antennas can be greatly simplified compared to the conventional approach. In the conventional approach the null field region of an equivalence problem is typically filled with a conductor, effectively short-circuiting the aperture and the electric surface current density everywhere. The remaining aperture magnetic surface current density, which is known, then radiates in the presence of the conductor and the Green's function associated with each particular antenna configuration has to be derived, usually a very cumbersome process. In the proposed technique a conductor is again placed within *S*, but with an infinitesimal small distance between the conductor and *S*. The image of the electric current density on *S* is shown to be induced on the conductor and the free space radiation integrals can now be used to solve the radiation problem. Examples are presented to prove the new technique and to demonstrate the mechanics of the equivalence principle when applied to aperture antenna problems.

Index Terms — Aperture antennas, aperture theory, equivalence principle, horn antennas, image theory, reflector antennas, slot antennas.

I. INTRODUCTION

This paper is intended to augment a technique published by the author in 2003 [1] through which radiation from arbitrarily shaped aperture antennas can be calculated by means of the free space radiation integrals, circumventing the need to derive problem-specific Green's functions as stated in most textbooks on the topic. The technique is based on the placement of a conductor in the null field region of a surface equivalence problem to "short-circuit" the aperture, and in [1] the author merely conjectured how the process should be interpreted from a mathematical point of view. In this paper it is demonstrated through an example that the author's initial assumptions were valid, and the implementation and limitations of the technique are discussed through additional examples. Whereas only radiated fields were presented for the examples discussed in [1], this paper focusses specifically on the induced current densities in the aperture region of the free space equivalence problem. Through the examples it is shown that the short-circuited aperture indeed reproduces the original aperture fields as would be required.

Figure 1 (a) depicts a physical aperture antenna radiating in free space (two-dimensional, for the sake of simplicity). The surface equivalence principle [2,3] can be applied to replace the physical antenna with equivalent electric and magnetic surface current densities radiating in free space, as shown in Fig. 1 (b). The equivalent electric and magnetic surface current densities are defined by (1) and (2), respectively, with $\hat{\mathbf{n}}$ a unit vector normal to *S*, pointing towards Region 1. The magnetic current density is zero everywhere except in the aperture region.

The electromagnetic fields external to *S* are equal to the electromagnetic fields in the original problem, but the fields internal to *S* are selected to be zero (Love's equivalence [4]). The sources $\mathbf{J_s}$ and $\mathbf{M_s}$ in Fig. 1 (b) radiate in an unbounded medium (same μ,ε everywhere) and can be used in conjunction with the free space radiation integrals (two-dimensional) in (3) and (4) to calculate the fields both regions of Fig. 1 (b). In Equations (3) and (4) *f* is the frequency, λ the wavelength, $\omega=2\pi f$ the angular frequency, k=$2\pi/\lambda$ the wavenumber, μ and ε the constituent parameters for the medium of propagation and *r* the distance from the integration point to the field evaluation point.

For many aperture antenna problems the distribution of the electric field in the aperture is known to good approximation, but not necessarily so the distribution and relative magnitude and phase of the magnetic field in the aperture, with slot antennas being a good example. *One would, therefore, try to redefine the problem such that only the magnetic current density needs to be taken into account as a source*;

$$\mathbf{J_s}= \hat{\mathbf{n}} \times \mathbf{H}_1, \qquad (1)$$

$$\mathbf{M_s} = -\,\hat{\mathbf{n}} \times \mathbf{E}_1, \tag{2}$$

$$\mathbf{E}(\mathbf{J_s}\,,\mathbf{M_s}) = -\frac{\omega\mu}{4}\int_S \mathbf{J_s}\, H_0^{(2)}(kr)\,\mathrm{d}S$$
$$+\frac{k}{4\omega\varepsilon}\int_S (\nabla_S \bullet\ \mathbf{J_s}\,)\,\hat{\mathbf{r}}\, H_1^{(2)}\,(kr)\,\mathrm{d}S$$
$$+\frac{\mathrm{jk}}{4}\int_S \mathbf{M_s} \times \hat{\mathbf{r}}\, H_1^{(2)}\,(kr)\mathrm{d}S, \tag{3}$$

$$\mathbf{H}(\mathbf{J_s}\,,\mathbf{M_s}) = -\frac{\omega\varepsilon}{4}\int_S \mathbf{M_s}\, H_0^{(2)}(kr)\,\mathrm{d}S$$
$$+\frac{k}{4\omega\mu}\int_S (\nabla_S \bullet\ \mathbf{M_s}\,)\,\hat{\mathbf{r}}\, H_1^{(2)}\,(kr)\,\mathrm{d}S$$
$$-\frac{\mathrm{jk}}{4}\int_S \mathbf{J_s} \times \hat{\mathbf{r}}\, H_1^{(2)}\,(kr)\mathrm{d}S\,. \tag{4}$$

Since the electromagnetic fields inside S are zero, the medium inside S can be replaced by a different medium without affecting the fields external to S [5]. If we fill the area inside S with an electric conductor as shown in Fig. 1 (c), the reciprocity theorem can be invoked to show that the electric current density $\mathbf{J_s}$ (including $\mathbf{J_s}{=}\mathbf{J_{ap}}$) will no longer produce any fields ("We can think of the conductor as shorting out the current" [6]), and we are left with a magnetic current density $\mathbf{M_s}{=}\mathbf{M_{ap}}$ impressed upon an electric conductor. However, since $\mathbf{M_s}$ no longer radiates in an unbounded medium, the free space radiation integrals of (3) and (4) can no longer be used to calculate the fields external to S. Consequently, as stated in two prominent antenna theory textbooks:

> "The introduction of the perfect conductor will have an effect on the equivalent source $\mathbf{J_s}$, and it will prohibit the use of [the free space radiation integrals] because the current densities no longer radiate into an unbounded medium. … *The problem of a magnetic current density radiating in the presence of an electric conducting surface must be solved. So it seems that the equivalent problem is just as difficult as the original problem itself.*" [7],

and

> "If a perfect conductor is placed along S, Js will vanish. The explanation is often given the electric current is 'shorted out' by the conductor. This leaves a magnetic current density Ms radiating in the presence of the electric conductor … these problems are difficult to solve as long as S is a general surface." [8].

What this implies is that the Green's function associated with the specific radiating geometry needs to be derived, typically a very cumbersome process that is limited to elementary geometries (see for example [9,10]). Furthermore, it is clear that some uncertainty exists about just how the conductor "shorts out" the electric current density.

We will next endeavour to show that it is possible to derive a new technique for solving the above problem

which "shorts out" $\mathbf{J_s}$, while still allowing the free space radiation integrals to be used (see also [1, Section 2]).

II. DERIVATION OF THE NEW TECHNIQUE

Since the electromagnetic fields within S (Region II) are zero, we can as before place an electric conductor within S, with the difference that the conductor does not fill Region II completely as shown in Fig. 1 (d). We can treat this as simply another equivalence problem in which the physical conductor, which is illuminated by external sources $\mathbf{J_s}$, $\mathbf{J_{ap}}$ and $\mathbf{M_{ap}}$, is replaced by an equivalent electrical surface current density $\mathbf{J_c}$ on C, with all current densities now radiating in free space. The induced electrical surface current density $\mathbf{J_c}$ in Fig. 1 (d) is equal to zero as all the electromagnetic fields within S are zero, but can still be expressed as:

$$\mathbf{J_c} = \mathbf{J_c}(\mathbf{J_s}) + \mathbf{J_c}(\mathbf{J_{ap}}) + \mathbf{J_c}(\mathbf{M_{ap}}) \equiv 0. \tag{5}$$

We next bring C infinitely close to S ($C{=}S^-$), with d small but not zero (i.e., $d \ll \lambda$). As proven by the reciprocity theorem, an electric current density radiating in the immediate presence of an electric conductor will produce no field. In terms of the configuration shown in Fig. 1 (d), and keeping in mind that all the current densities radiate in free space, this is mathematically speaking only possible if $\mathbf{J_c}(\mathbf{J_s}) \approx -\mathbf{J_s}$ at any point on the conducting part of S and likewise $\mathbf{J_c}(\mathbf{J_{ap}}) \approx -\mathbf{J_{ap}}$ in the aperture region. The fields radiated by $\mathbf{J_s} + \mathbf{J_c}$, external to S are calculated from (3) and (4) and can only be zero if $\mathbf{J_c} = -\mathbf{J_s}$. The "image" of $\mathbf{J_s}$ is therefore induced on the conductor that backs $\mathbf{J_s}$, irrespective of the shape of S.

With the electric source current densities having accordingly been cancelled everywhere on S, the problem in Fig. 1 (d) is reduced to the one shown in Fig. 1 (e), where $\mathbf{M_{ap}}$ induces $\mathbf{J_c}(\mathbf{M_{ap}})$ on S^-, which now is a closed electrical conductor. In other words, the aperture has been short-circuited with $\mathbf{M_{ap}}$ placed infinitely close to it in the aperture region as shown in Fig. 1 (e), and $\mathbf{J_c}(\mathbf{M_{ap}})$ is merely the electric current density it induces on C.

The magnetic surface current density $\mathbf{M_{ap}}$ is usually known for many aperture antennas and $\mathbf{J_c}$ can then be solved for by techniques such as the Electric Field Integral Equations (EFIE) and the Method of Moments (MoM) [11]. *Significantly, it is no longer necessary to derive the Green's function of the specific radiating structure*. Note that it does not matter whether the conductor is placed inside S on S^-, or on S with $\mathbf{M_{ap}}$ moved an infinitesimal distance outside S to S^+. The latter approach is often easier to implement as the radiating structure may be quite complex while the aperture field distribution typically is simple by comparison (see the horn antenna examples at the end). *This forms the premise of the new technique.*

One may ask whether the new technique will reproduce the original surface current densities $\mathbf{J_s}$ and $\mathbf{J_{ap}}$ on S^- and this is indeed what we can expect. From (5) we have:

$$\mathbf{J_c}(\mathbf{M_{ap}}) = -\mathbf{J_c}(\mathbf{J_s}) - \mathbf{J_c}(\mathbf{J_{ap}}), \qquad (6)$$

and as we have argued above, for d approximating zero,

$\mathbf{J_c}(\mathbf{J_s}) = -\mathbf{J_s}$ and $\mathbf{J_c}(\mathbf{J_{ap}}) = -\mathbf{J_{ap}}$ on C, which yields:

$$\mathbf{J_c}(\mathbf{M_{ap}}) = \mathbf{J}_s + \mathbf{J_{ap}}, \qquad (7)$$

or to be more precise, $\mathbf{J_c}(\mathbf{M_{ap}}) = \mathbf{J_{ap}}$ in the aperture region of S and zero elsewhere, and $\mathbf{J_c}(\mathbf{M_{ap}}) = \mathbf{J_s}$ in the conducting region of S and zero elsewhere.
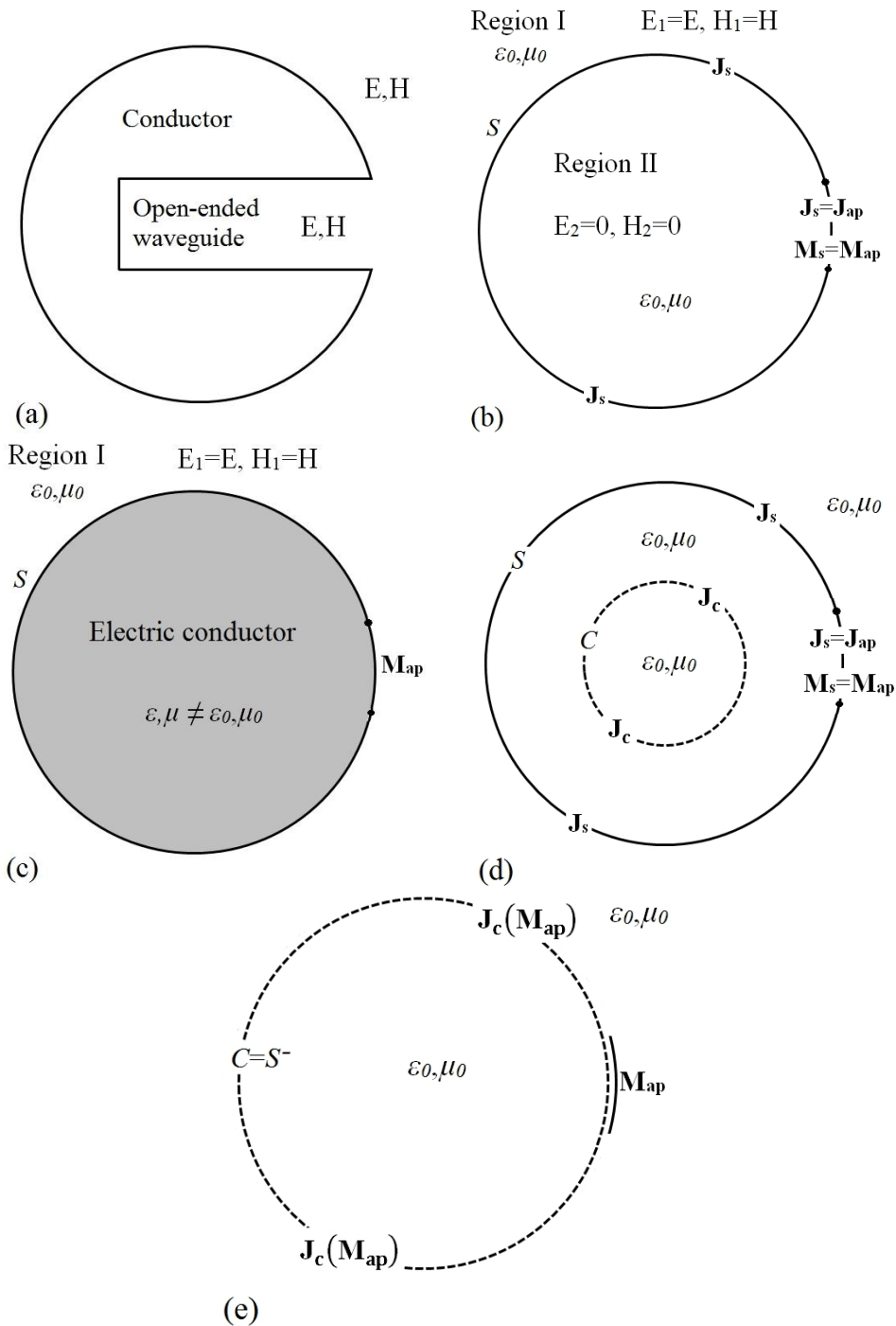

Fig. 1. Application of the equivalence principle to an aperture antenna problem.

III. SHORT-CIRCUITING AN ELECTRIC SURFACE CURRENT DENSITY RADIATING IN FREE SPACE

In order to prove the validity of the new technique, we will first demonstrate through an example that when an electrical conductor is brought infinitely close to an electric surface current density $\mathbf{J_s}$ defined on an arbitrarily shaped surface S, radiating in free space, the oppositely directed current density will be induced on the conductor ($\mathbf{J_c} = -\mathbf{J_s}$) and $\mathbf{J_s}$ will effectively be short-circuited. No electromagnetic fields will be radiated by the combination of $\mathbf{J_s}$ and the current density $\mathbf{J_c}$ on the conductor. Although this sounds logical, it is important to note that the conductor can be replaced by the negative image of $\mathbf{J_s}$ everywhere on S, although classical image theory [12] does not apply to the problem in any sense.

As an example, Fig. 2 depicts a surface current density $\mathbf{J_s}$ superimposed onto a circular surface S of radius R=λ, with an electrical conductor of radius r having been placed at the centre of S. The gap between S and the conductor is given by d=R-r. The surface current density $\mathbf{J_s}$ is defined by (8) to (10) and does *not* produce a zero field inside S. Note that the phase function α is calculated first for $0 \leq \varphi \leq \pi$, from which the magnitude function J is calculated over the same sector. As indicated by (10), the current in the sector $-\pi \leq \varphi \leq 0$ is numerically duplicated from the $0 \leq \varphi \leq \pi$ sector. Placing a conductor inside S will therefore affect the total radiated field.

The induced surface current density $\mathbf{J_c}$ and the total radiated field were calculated by means of the EFIE and MoM for r=0 (i.e., no reflector, denoted 'Source' in the plots), r=0.5λ, r=0.95λ and r=0.999λ, respectively. Figure 3 shows the magnitude and phase of the calculated electric current density $\mathbf{J_c}$ for the abovementioned reflector radii, and Fig. 4 the radiated far field (calculated at 100 m at f=2 GHz). It is clear that as $d\rightarrow0$ (i.e., $r\rightarrow$R), $\mathbf{J_c} \rightarrow -\mathbf{J_s}$ and the total radiated field given by $\mathbf{J_s} + \mathbf{J_c}$ tends to zero (already being 45 dB down from the case where r=0). In Fig. 3 (b) a value of +180° was added to the phase of $\mathbf{J_c}$ in order to facilitate a direct overlay of the curves.

$$\alpha(\varphi) = \varphi + \pi \cos 2\varphi, \quad 0 \leq \varphi \leq \pi, \qquad (8)$$

$$J(\varphi) = \left| \cos\left(\frac{\alpha(\varphi)}{3}\right) \right|, \ 0 \leq \varphi \leq \pi, \qquad (9)$$

$$\mathbf{J_s}(\varphi) = J(\varphi)e^{j\alpha(\varphi)}, \ \ \mathbf{J_s}(-\varphi) = \mathbf{J_s}(\varphi). \qquad (10)$$

We will next discuss the application of the new technique through several examples.
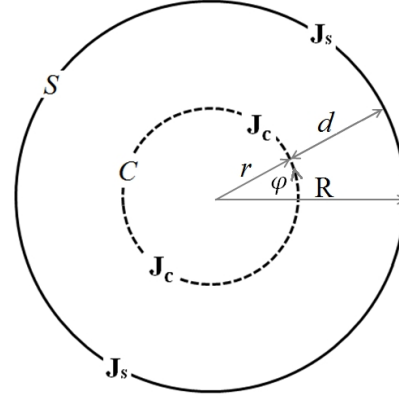
Fig. 2. $\mathbf{J_s}$ superimposed onto a circular surface S with conductor C placed inside S, $r\rightarrow$R.
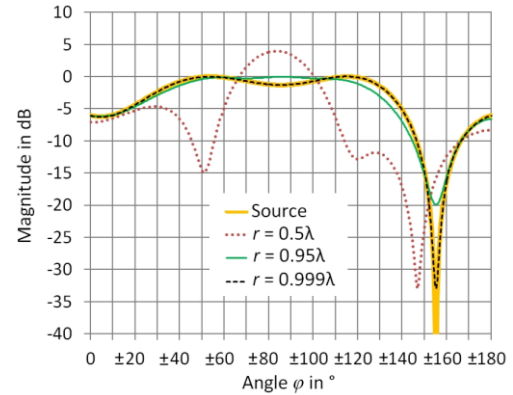
(a) Magnitude
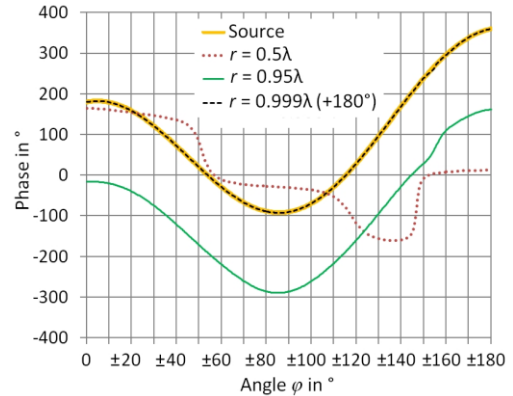
(b) Phase

Fig. 3. Magnitude and phase of $\mathbf{J_c}$ for r=0, r=0.5λ, r=0.95λ and r=0.999λ.
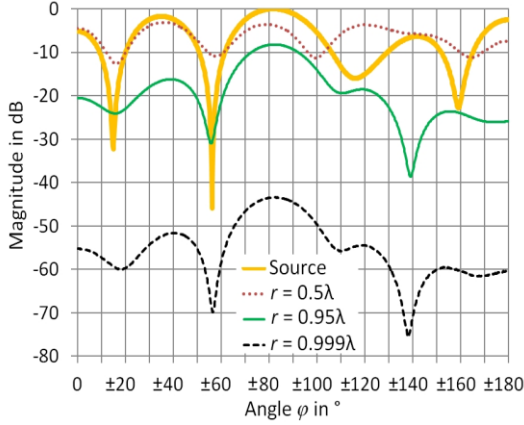
Fig. 4. Radiated patterns for $r=0$, $r=0.5\lambda$, $r=0.95\lambda$ and $r=0.999\lambda$.

IV. EXAMPLE 1 – A LINE SOURCE RADIATING IN FREE SPACE

Perhaps the simplest example for demonstrating how the new technique can be used is the case of a line source radiating in two-dimensional free space, as shown in Fig. 5. The electric and magnetic source fields at distance r from the source are expressed by Equations (11) and (12), respectively:

$$\mathbf{E}_i(r) = \frac{1}{\sqrt{r}} e^{-jkr}\, \hat{\mathbf{z}} \ = E_i(r)\, \hat{\mathbf{z}}, \qquad (11)$$

$$\mathbf{H}_i(r) = -\frac{1}{\eta} E_i(r)\, \hat{\boldsymbol{\varphi}}. \qquad (12)$$

In (12) η represents the free space wave impedance.

An equivalent surface S can now be placed around the line source and together with the surface current densities $\mathbf{J}_{s1}$ and $\mathbf{M}_{s1}$, it will produce the true fields with S and a null field external to S. For external equivalence, the surface current densities $\mathbf{J}_{s2}=-\mathbf{J}_{s1}$ and $\mathbf{M}_{s2}=-\mathbf{M}_{s1}$ will produce null fields internal to S and the original (true) fields external to S. For the sake of simplicity, we define surface current densities $\mathbf{J}_1=-\mathbf{J}_{s1}$ and $\mathbf{M}_1=-\mathbf{M}_{s1}$ to produce the external fields (Region 1 as defined in Fig. 1). Two examples were considered, one in which S is a circle and the other in which S is a square with the line source at its centre. Note that since $\mathbf{J}_s$ is z-directed, the surface divergence term in (3) is zero. The surface divergence integral in (4) can also be neglected for slowly varying $\mathbf{M}_s$ as the coefficients of the two integrals involving $\mathbf{M}_s$ differ by a factor of $k=2\pi/\lambda$ and for evaluation points directly below $\mathbf{M}_s$, we have $\hat{\mathbf{n}} = -\hat{\mathbf{r}}$, so that from (1) and (4) the cross product will be zero. As before, an electric conductor C is next placed inside S and brought infinitely close to S.

The free-space fields can be viewed as aperture fields and, in accordance with the new technique, S can be viewed as a conductor ($\hat{\mathbf{n}} \times \mathbf{E} = 0$ on its surface) with $\mathbf{J}_c$ on S and $\mathbf{M}_{s2}$ having been placed an infinitesimally

small distance outside S.

We first consider the case where S is circular, $f = 3$ GHz and $r = R_o = 3\lambda$. From Equations (1), (2), (11) and (12) we have:

$$\mathbf{J}_1 = -\frac{1}{\eta} E_i(R_o)\, \hat{\mathbf{z}} \ = -46.29 \text{ dB} \angle 180° \, \hat{\mathbf{z}}, \qquad (13)$$

$$\mathbf{M}_1 = + E_i(R_o)\, \hat{\boldsymbol{\varphi}} \ = +5.23 \text{ dB} \angle 0° \, \hat{\boldsymbol{\varphi}}, \qquad (14)$$

everywhere on S, due to the symmetry of the problem. With $d=0.03\,\lambda$, the value for $\mathbf{J}_c$ calculated by means of the MoM (the author used a rather elementary pulse basis function with point matching scheme) was $\mathbf{J}_c = -46.19$ dB $\angle 168°\, \hat{\mathbf{z}}$. Note that since $\mathbf{M}_1$ was used as the source and it was placed a distance d away from the equivalent surface S (see Fig. 6), one should expect a phase difference between $\mathbf{J}_1$ and $\mathbf{J}_c$ of about $-kd = -10.8°$, which is indeed the case ($180°-10.8°=169.2°$). Since the source surface current density $\mathbf{M}_s$ will typically be approximated by segments, a general rule of thumb for the ratio between d and $\Delta\mathbf{M}$, the length of the segments, is $\Delta\mathbf{M} \le d$. Conversely, the distance between integration or sampling points on $\mathbf{M}_s$ should be smaller than d.

We next consider the case where S takes the form of a square that replaces the circle with radius R_o, as shown in Fig. 6. In this case (13) and (14) still hold where r = R_o, but the equivalent surface current densities $\mathbf{J}_1$ and $\mathbf{M}_1$ are no longer uniform on S. With r(x,y) and $\hat{\boldsymbol{\varphi}}$ as defined in Fig. 5, we can derive the following equations for the right hand side of the square, and similar equations for the other three sides of the square:

$$r = r(x,y) = \sqrt{x^2+y^2}, \qquad (15)$$

$$\hat{\mathbf{n}} = \hat{\mathbf{x}}, \qquad (16)$$

$$\hat{\boldsymbol{\varphi}} = -\sin(\varphi)\, \hat{\mathbf{x}} + \cos(\varphi)\, \hat{\mathbf{y}}, \qquad (17)$$

$$\mathbf{J}_1 = \hat{\mathbf{n}} \times \mathbf{H}_i(r) = -\frac{1}{\eta} E_i(r) \cos(\varphi)\, \hat{\mathbf{z}}, \qquad (18)$$

$$\mathbf{M}_1 = - \hat{\mathbf{n}} \times \mathbf{E}_i(r) = E_i(r)\, \hat{\mathbf{y}}. \qquad (19)$$
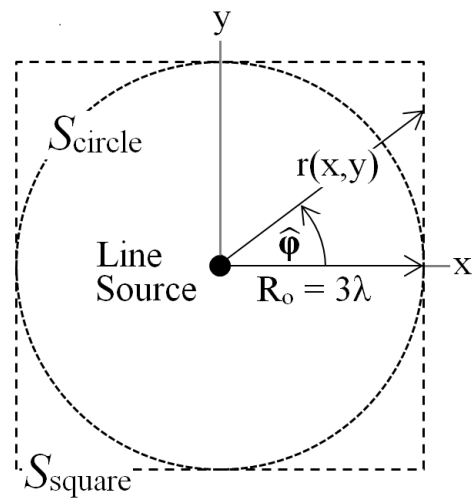

Fig. 5. Line source in two-dimensional space with S circular and square.
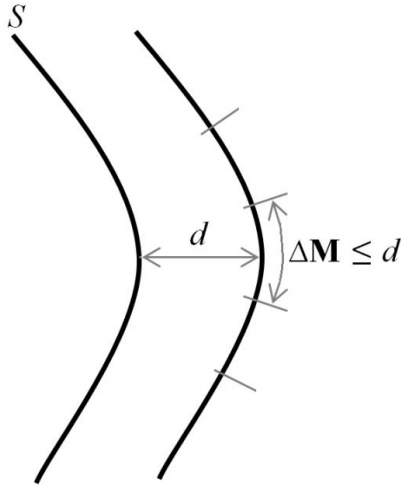
Fig. 6. Rule of thumb for ratio of d to $\Delta\mathbf{M}$.

Figure 7 shows the geometrical optics current density from (18) as well as the MoM current density calculated from $\mathbf{M_1}$ in (19) as backed by a conductor a distance d inside S. The erratic behaviour of the current density amplitude at the corners is most likely due to the field distribution at the 90° corners, which would generate a diffraction term for d not equal to zero. The phase difference of about 10° is like before due to the distance d between $\mathbf{M_1}$ and the conductor on which $\mathbf{J_1}$ is induced.

From these graphs it is clear that $\mathbf{M_1}$ backed by a perfect electrical conductor does indeed reproduce the original free space electrical surface current density $\mathbf{J_1}$ on S.

It is instructive look at the total fields radiated by $\mathbf{J_1}$ and $\mathbf{M_1}$ as well (integration is performed along the entire length of S). For this example a cross section of the equivalent surface was taken as shown in Fig. 8.

Inside S we expect the fields radiated by $\mathbf{J_1}$ and $\mathbf{M_1}$ to add up to zero, and to the true (geometrical optics) fields outside S. This is indeed the case, as shown in Figs. 9 (a) to 9 (c). In these figures 'Original' designates the electric field as calculated from (11), 'J&M' the results obtained from the geometrical optics expressions for $\mathbf{J_1}$ and $\mathbf{M_1}$, 'Circle + SC' the MoM $\mathbf{J_1}$ obtained by placing $\mathbf{M_1}$ on a concentric circle around the line source and backing (short-circuiting) it with a conductor, and 'Square + SC' the same for the square surface. As expected, the fields in the null region are not identically equal to zero, most likely due to the limitations of the pulse basis function with point matching scheme used by the author, and phase differences between $\mathbf{J_1}$ and $\mathbf{M_1}$.

Inside (left) of S, $\mathbf{J_1}$ and $\mathbf{M_1}$ will more or less add correctly in phase as $\mathbf{J_1}$ already lags $\mathbf{M_1}$ in phase by $-kd$, but when $\mathbf{M_1}$ radiates inward, it will also have undergone a phase change of $-kd$ (see Fig. 10). However, for external radiation $\mathbf{J_1}$, which already lags by $-kd$, will

undergo another phase shift of $-kd$ before reaching $\mathbf{M_1}$. The new technique will, therefore, introduce a local phase difference of $-2kd$ between $\mathbf{J_1}$ and $\mathbf{M_1}$, which will have some effect on the total radiated fields. Nevertheless, the effect will still be almost negligible when the closed surface integration is performed as is evident from Fig. 9 (c), which shows the magnitude and phase differences between MoM calculated results and the original field calculated form (11).
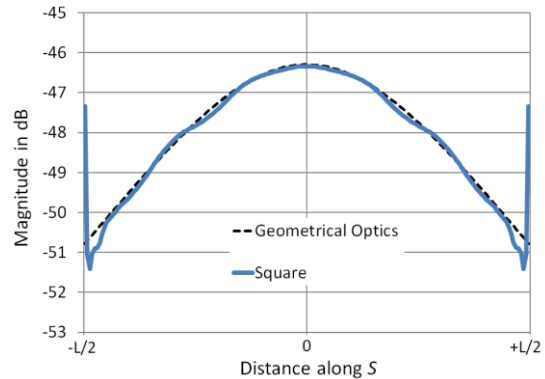

(a) Magnitude
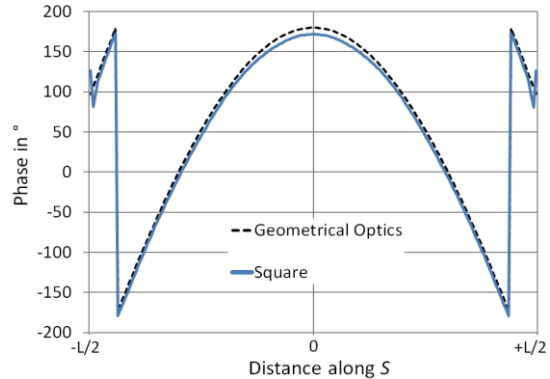
(b) Phase

Fig. 7. Magnitude and phase distribution of $\mathbf{J_1}$ along one side of the square.
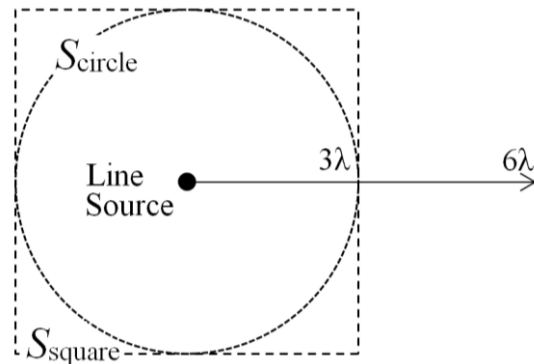
Fig. 8. Cross section through S for electric field strength calculation.

(a) Magnitude

(b) Phase

(c) Relative magnitude and phase errors
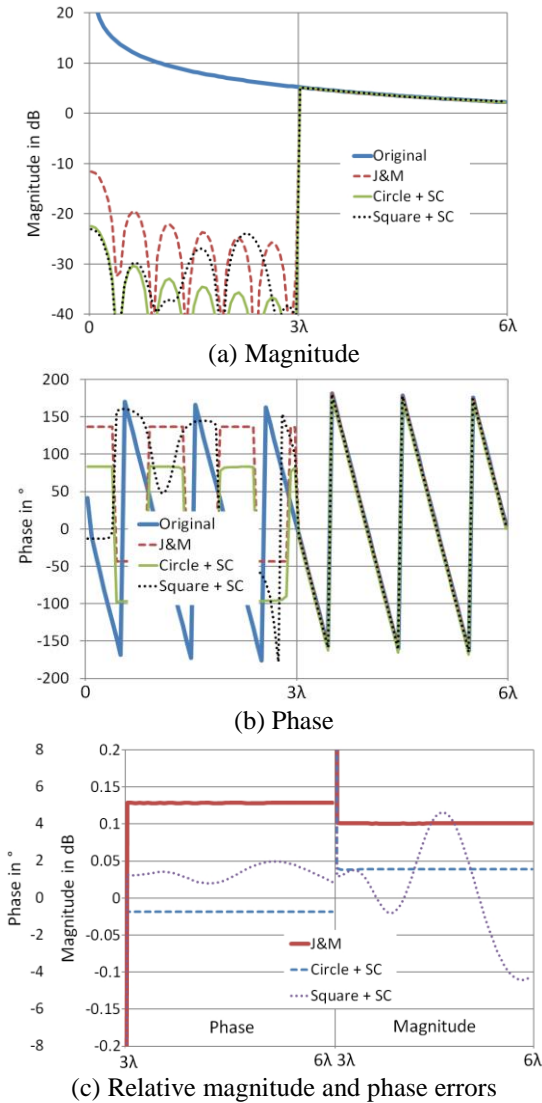
Fig. 9. Magnitude, phase and errors between GO field and MoM calculated electric field along cross section through S.

(a)
Original problem

(b)
M_1 moved a distance d to the right of S
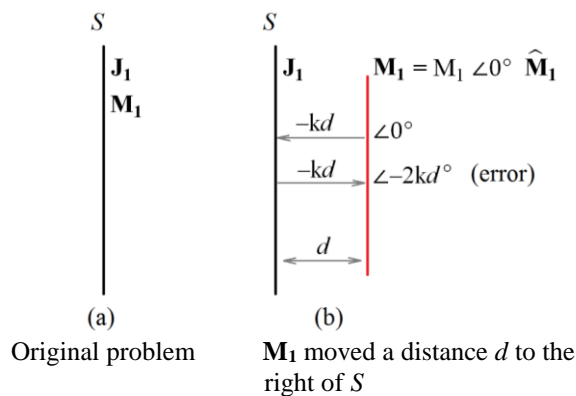
Fig. 10. Phase error in field component radiated by J_1 in new technique.

V. EXAMPLE 2 – REFLECTOR WITH LINE SOURCE FEED

The next example demonstrates how the new technique can be used with arbitrarily shaped aperture fields and radiating structures. The basic problem is depicted in Fig. 11 (a), where a line source illuminates a parabolic reflector with dimensions $D=10\lambda$, $F=1\lambda$, which is evaluated at $f=10$ GHz. The problem was initially solved by means of the MoM, following which an artificial circular equivalent surface S was introduced as shown in Fig. 11 (b), with $r=3.02\lambda$. The electric field along this surface was calculated by means of the MoM and was then converted to the magnetic source current density M_1. S was then "short-circuited" (i.e., treated as a continuation of the reflector surface), and M_1 was moved a distance $d=0.05\lambda$ away from S, in accordance with Fig. 1 (e), and the equivalent electric current density J_c on S was calculated by means of the MoM.

(a) Original problem

(b) With circular equivalent surface
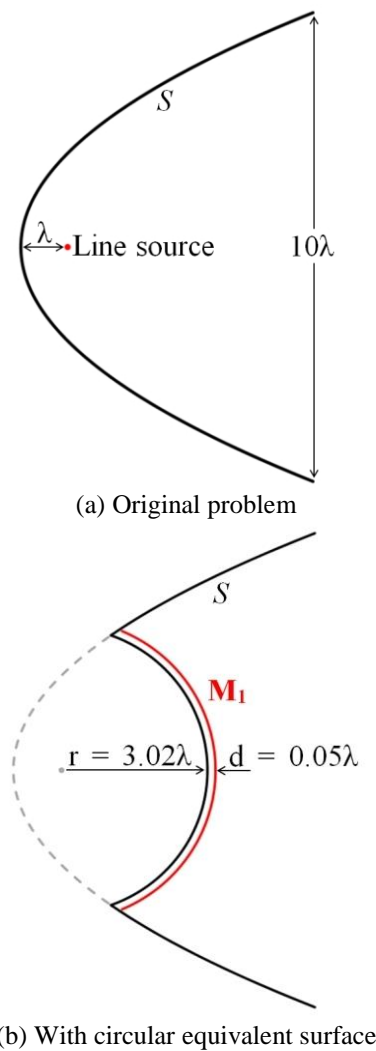
Fig. 11. Parabolic reflector with artificial equivalent aperture surface.

It is relatively straightforward to calculate the geometrical optics reflected electric and magnetic fields on S as depicted in Fig. 12, from which the geometrical optics magnetic and electric equivalent current densities $\mathbf{M_{GO}}$ and $\mathbf{J_{GO}}$ at point (x,y) can be calculated as:

$$\mathbf{M_{GO}} = \left(\frac{e^{-jkl_a}}{\sqrt{l_a}} - \frac{e^{-jk(l_b+l_c)}}{\sqrt{l_b}} \right) \hat{\boldsymbol{\varphi}}, \qquad (14)$$

and

$$\mathbf{J_{GO}} = \left(-\frac{e^{-jkl_a}}{\eta\sqrt{l_a}} + \frac{e^{-jk(l_b+l_c)}}{\eta\sqrt{l_b}} \cos\varphi \right) \hat{\mathbf{z}}. \qquad (15)$$
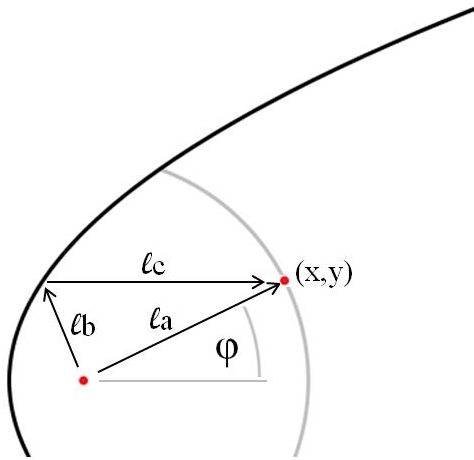

Fig. 12. Geometrical optics ray paths for direct and reflected fields.

Figures 13 and 14 show the magnitude and phase plots of the MoM calculated magnetic and electric current densities $\mathbf{M_1}$ and $\mathbf{J_c}$, respectively, compared to the geometrical optics calculated current densities $\mathbf{M_{GO}}$ and $\mathbf{J_{GO}}$. The difference between the MoM and GO current densities in the centre region can most likely be attributed to the fact that diffracted fields from the edges of the reflector had been ignored in the GO calculations (these would add in phase along the axis of the reflector). At the magnitude peaks in Fig. 14 (a) the difference between the MoM and GO results is, however, very small and the phase difference in Fig. 14 (b) at these points is about -18.6°, as can be expected for d=0.05λ (-kd=-18.0°). The abrupt discontinuity in the electric surface current density of (1) at the transition from the reflector to the circular region is due to the abrupt change in the direction of $\hat{\mathbf{n}}$ at this point. It will become less as the segmentation (the distance between sampling points) is made smaller.

Note that the x-axis in these graphs reflects only *the number of sampling points*, of which the density is greater in the centre of the parabola, and not the true distance along S. The Physical Optics current density

[13] (PO), which is given by the approximation $\mathbf{J_{PO}}=2\,\hat{\mathbf{n}} \times \mathbf{H_i}$, is also shown in Fig. 14, overlaid with the MoM current density as calculated outside the aperture area. The magnitude difference between the PO and MoM results is typically less than 0.5 dB and in fact reduces even further as the electrical size of the parabola is increased.

It is of interest that the stationary phase solution of the radiation integrals associated with $\mathbf{J_{PO}}$ can be shown to yield the geometrical optics reflected fields [14] as used to derive (14) and (15).

This example again confirms that a short-circuited magnetic current density radiating in free space induces the corresponding free space electric current density on the conducting surface, which also radiates in free space. It would be near impossible to derive a Green's function for the geometry shown in Fig. 11 (b).

Figure 15 shows the far field radiation patterns for the original configuration of Fig. 11 (a) and the configuration with the circular equivalent surface shown in Fig. 11 (b), respectively. Despite the two approaches being fundamentally different, the agreement is excellent.
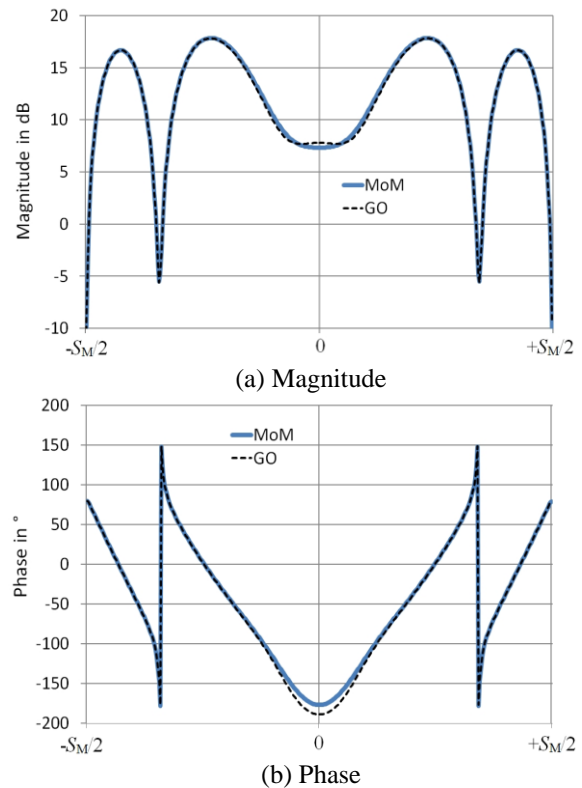

(a) Magnitude

(b) Phase

Fig. 13. Magnitude and phase of calculated $\mathbf{M_1}$ in circular aperture region.
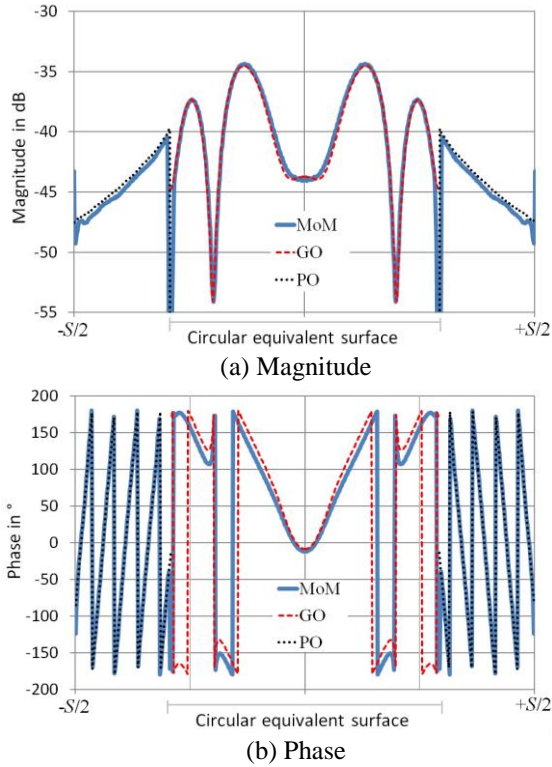
(a) Magnitude

(b) Phase

Fig. 14. Magnitude and phase distribution of $\mathbf{J_c}$ along S for parabolic reflector example.
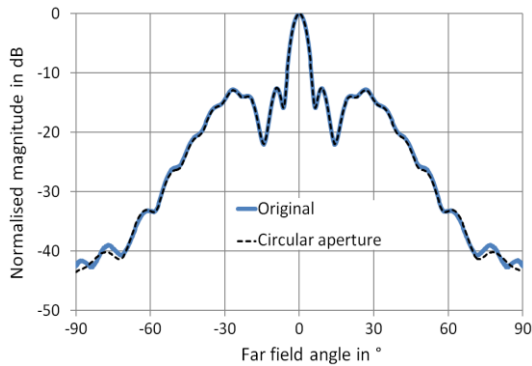
Fig. 15. Far field radiation patterns for parabolic reflector example.

VI. HORN ANTENNA EXAMPLES

It is important to note some of the practical applications of the new technique. As an example, radiation from an X-band flared horn antenna with waveguide dimensions W_W=22.86 mm and W_H=10.16 mm, aperture dimensions A_W=22.86 + 2x20 = 62.86 mm and A_H=10.16 + 2x20 =50.16 mm, and length L=20 mm (Fig. 16) was calculated by means of 2D and 3D (FEKO [15]) simulation software. In the 2D case, the waveguide aperture was short-circuited and the equivalent magnetic current densities $\mathbf{M_W}$=cos(y/W_W*π)$\hat{\mathbf{y}}$ for −W_W/2 ≤ y ≤

+W_W/2 and $\mathbf{M_H}$=$\hat{\mathbf{z}}$ for −W_H/2 ≤ y ≤ +W_H/2, were placed a distance d=0.02λ to the right of the short-circuited waveguide aperture, respectively.

Note that for the 2D calculations the E-plane and H-plane problems were solved independently of each other. The 3D horn antenna was fed by a waveguide which was excited with the FEKO rectangular waveguide source model. As shown in Fig. 17, the correlation between the 2D patterns and the 3D principal plane patterns is very good despite the simplifications made from the 3D to the 2D models. This example also serves to demonstrate the usefulness of 2D simulation to obtain first-order design results for problems that can be reduced to 2D analysis.
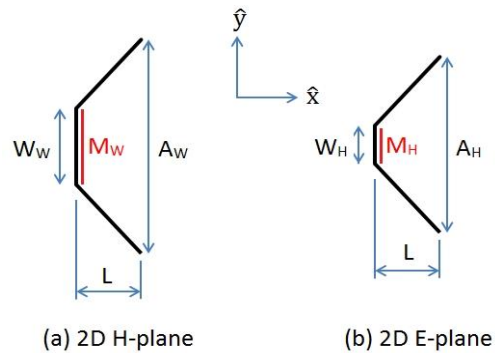
(a) 2D H-plane   (b) 2D E-plane
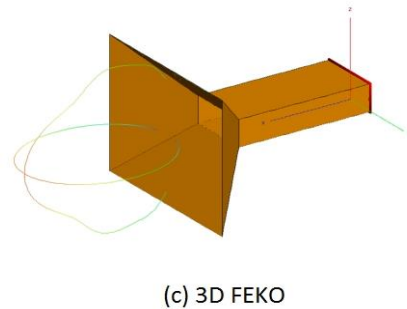
(c) 3D FEKO

Fig. 16. 2D and 3D models of X-band flared horn antenna.
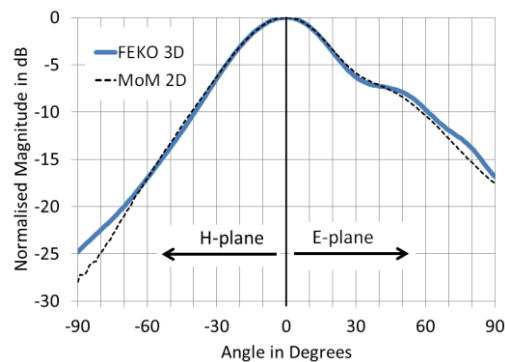
Fig. 17. E- and H-plane radiation patterns of an X-band flared horn antenna.

VII. CONCLUSION

The aim of this paper is to augment an equivalence principle-based technique earlier published by the author, for simplifying the calculation of radiation from arbitrarily shaped aperture antennas when the electric field distribution in the aperture is known. Traditionally the Green's function specific to the problem had to be derived, but with the new technique the aperture can be short-circuited and the free space Green's functions (i.e., the free space radiation integrals) can be used to calculate the fields radiated from the aperture in the presence of the arbitrarily shaped surrounding antenna structure. The validity of this technique is demonstrated and the examples presented provide valuable insight into the mechanics of the equivalence principle and the concept of placing a conductor in the null field region of surface equivalence problems.

The author would also, in conclusion, like to present a brief overview of the arduous route the development of the new technique had taken. During the mid-1990s he had developed an elementary Electric Field Integral Equation free space MoM code for the design of certain types of antennas. As an afterthought he decided to add aperture antennas as well, because of its apparent simplicity. The problem was that although the electric field in the aperture is usually known, the magnetic field is not, and he soon found that for certain examples completely inaccurate results were obtained. Through trial and error he discovered that when the aperture is short-circuited and $\mathbf{M_s}$ is placed a small distance away from it, the free space calculated results agreed perfectly with measured and theoretical results. This was in direct contrast to all the textbooks he could find at the time, in which it was stated that the free space radiation integrals could not be applied to such problems, as discussed above.

The author submitted a paper to a prominent antenna journal in August of 1996, but it was eventually rejected in March 1998, in hindsight for perfectly valid reasons. An opportunity then came along to present a paper on the topic at a local symposium in South Africa in September 1998 [16], but there were no experts in the field who could venture an opinion either for or against it. The author then presented the same topic at the international AP Symposium in Orlando, Florida, in 1999 [17], to which he invited several recognised experts in the field of electromagnetic theory. At both of these presentations the author proceeded to show through examples that it is possible to use the free space radiation integrals to calculate radiation from arbitrarily shaped aperture antennas, and presented an admittedly somewhat heuristic mathematical approach in an attempt to prove the validity of the new technique. More importantly, however, the author *mistakenly* argued that the placement of a conductor in the null field of an equivalence problem was incorrect, as no current would

be induced on the conductor and no 'image' could therefore ever be generated. At that stage he had not realised that although the total induced current would be zero in the null region, it is comprised of the sum of more than one source, as expressed by (5), and that the electric current density would indeed be short-circuited as discussed by Harrington and others. It was in fact this realisation that had eventually led to the technique presented in this paper ([1, Section 2], Section II above). Needless to say, no support for or interest in the proposed technique was expressed during these presentations.

The author then derived a new theoretical 'proof' of the new technique *based purely on a mathematical manipulation of the free space radiation integrals* [1, Section 3], that did not rely on the placement of a conductor in the null field of the equivalence problem. He next contacted Prof. Sembiam Rengarajan, whom he had met before and who generously agreed to work through the paper the author intended to submit to the *IEEE Antennas and Propagation Society Magazine*. After a couple of months of back-and-forth correspondence, it was agreed that the paper was probably suitable for submission to the *Magazine*, which the author proceeded to do. The author was soon afterwards contacted by Prof. Joseph Mautz, who had been appointed as Reviewer of the paper, but was concerned that he might not be able to completely follow the author's arguments. He graciously suggested that the author and he correspond about the contents of the paper, which resulted in a series of friendly battle-of-wits exchanges until he was finally prepared to accept the paper for publication (see [1]).

Due to an apparent lack of recognition of his proposed technique, the author decided to take another look at it during the latter half of 2015, with the emphasis on the calculation of the actual induced electrical current density in the short-circuited aperture, as demonstrated by the examples presented above. It was during this process that he managed to demonstrate the validity of the "short-circuiting" concept (Section II), which is now reconciled with the conductor-in-the-null-field approach presented in practically all antenna textbooks that deal with aperture theory. In his opinion the value of this paper is not only to present confirmation of the new technique he had discovered earlier, but also to provide students with additional insight into the application of the equivalence principle to a specific class of antenna radiation problems.

REFERENCES

[1] A. J. Booysen, "Aperture theory and the equivalence principle," *IEEE Antennas and Propagation Magazine*, vol. 45, no. 3, pp. 29-40, June 2003.

[2] R. F. Harrington, *Time-Harmonic Electromagnetic Fields*. New York: McGraw-Hill, pp. 106-113,

1961.

[3] K.-M. Chen, "A mathematical formulation of the equivalence principle," *IEEE Trans. Microw. Theory Techn.*, vol. 37, no. 10, pp. 1576-1581, Oct. 1989.

[4] A. E. H. Love, "The integration of equations of propagation of electric waves," *Phil. Trans. Roy. Soc. London, Ser. A*, 197, pp. 1-45, 1901.

[5] *Time-Harmonic Electromagnetic Fields*, pp. 108-109.

[6] *Ibid.*, p. 109.

[7] C. A. Balanis, *Antenna Theory: Analysis and Design*. 4th ed., Hoboken, New Jersey: John Wiley & Sons, Inc., pp. 642-643, 2016.

[8] W. L. Stutzman and G. A. Thiele, *Antenna Theory and Design*. 3rd ed., Hoboken, New Jersey: John Wiley & Sons, Inc., p. 346, 2013.

[9] C. A. Balanis, *Advanced Engineering Electromagnetics*. New York: John Wiley & Sons, ch. 14, 1989.

[10] Y. Svezhentsev, "Mixed-potential reen's function of an axially symmetric sheet magnetic current on a circular metal surface," *Progress In Electromagnetics Research*, *PIER*, 60, pp. 245-264, 2006.

[11] R. F. Harrington, *Field Computation by Moment Methods*. Wiley-IEEE Press, 1993 reprint of the 1968 ed.

[12] *Advanced Engineering Electromagnetics*, Section 7.4.

[13] *Time-Harmonic Electromagnetic Fields*, pp. 127-128.

[14] A. J. Booysen, "On the equivalence of the geometrical-optics reflected fields and the stationary-phase solution of the associated radiation integrals," *IEEE Antennas and Propagation Magazine*, vol. 44, no. 5, pp. 120-123, Oct. 2002.

[15] FEKO (Altair Hyperworks), ver. 14, www.feko.info, 2016.

[16] A.J . Booysen, "Aperture theory and the equivalence theorem," *Proceedings of the 1998 South African Communications and Signal Processing Conference*, Rondebosch, Cape Town, pp. 353-358, Sept. 1998.

[17] A. J. Booysen, "Aperture theory and the equivalence theorem," *IEEE Antennas and Propagation Society International Symposium*, Orlando, Florida, vol. 2, pp. 1258-1261, July 1999.

Adriaan J. Booysen received his Ph.D. in Electronic Engineering (Electromagnetics) from the University of Pretoria in 1990. He has since worked at the Antenna Systems Group of Saab Grintek Defence, initially as a Development Engineer and currently as Head of the group. Although his main interest is the design and manufacture of microwave antennas for a variety of EW platforms, he has throughout his career maintained a keen interest in antenna theory and design. Booysen is a Senior Member of the *Institute of Electrical and Electronics Engineers* and has published a number of papers on antenna and electromagnetic theory.